Influence of the parasitics on the time delayed Chua's circuit

M. Biey, F. Bonani, M. Gilli and I. Maio
Politecnico di Torino, Dipartimento di Elettronica,
Corso Duca degli Abruzzi 24, 10129 Torino, Italy,
Phone (39) 11-5644025 Fax (39) 11-5644099 E-mail biey@polito.it.

Abstract - **The time-delayed Chua's circuit (TDCC) can be considered as a paradigm for studying the effect of the parasitics on circuits described by difference equations. This paper discusses the effect of a *small* capacitor C on the dynamics of the TDCC through the theoretical analysis of the characteristic equation in each region of linearity. The main result is that any TDCC which exhibits the period-adding route to chaos for $C = 0$, still continues to present this phenomenon even if a small capacitor C is added to the circuit.**

I. Introduction

A great deal of interest has been recently aroused by the analysis and exploitation of circuits implementing chaotic difference equations [1]. The dynamics of these circuits is strongly influenced by the presence of reactive parasitics, which may result in unexpected behaviors [2].

In this work, we analyze the effect of the capacitor C in the Time Delayed Chua's Circuit (TDCC) shown in Fig. 1. This circuit, for $C = 0$, is described by a *difference* equation which may exhibit chaotic behaviors akin to those observed in *dry* systems, *i.e.* in absence of viscosity [2]. For $C \neq 0$, the TDCC dynamics, now defined by a nonlinear *differential-difference* equation, can be completely different and is very difficult to be studied due to the lack of a comprehensive analytical treatment of these equations. So far, the TDCC has been studied only through numerical simulations [5; 6].

The next section is devoted to a complete description of the circuit equations, while Sec. III contains a qualitative analysis of the circuit dynamics supported by numerical simulations.

II. Circuit equations

The TDCC and the Chua's diode characteristic are shown in Fig. 1 and 2, respectively, where the variables involved in the analysis are also defined. The parameters of the circuit are the round trip delay T and the characteristic impedance Z of the transmission line, the slopes m_0, m_1, m_{-1} and the switching voltage B_p of the Chua's diode, the source voltage E, and the lumped linear elements C and G.

The equations describing the lumped part of the network are:

$$\begin{cases} C\dfrac{dv}{dt} + g(v(t) - E) + i'(t,0) = 0 \ , \\ G[v(t) - v'(t,0)] = i'(t,0) \ , \end{cases} \tag{1}$$

where $g(\cdot)$ is the piecewise linear function represented

0-7803-31-09-5/96/$5.00

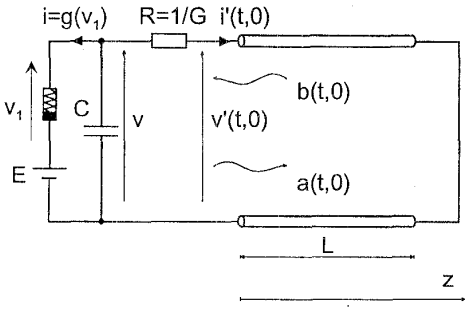

Fig. 1. Time-delayed Chua's circuit.

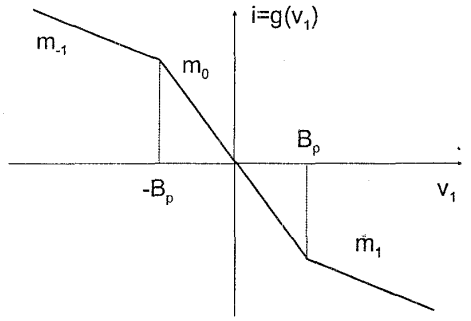

Fig. 2. Current-voltage characteristics of Chua's diode.

in Fig. 2. As a consequence, the TDCC is a piecewise linear circuit with three regions of linear operation, selected by the value of $v_1 = v - E$. For $v_1 < -B_p$, $|v_1| \leq B_p$ and $v_1 > B_p$, the Chua's diode operates on its leftmost, central and rightmost linear branch, respectively. In the following, these regions of linear operation are indicated by $\mathcal{R}_{-1}$, $\mathcal{R}_0$ and $\mathcal{R}_1$. In the linear region $\mathcal{R}_j$ the function $g(v_1)$ of Fig. 2 is expressed by $g(v_1) = m_j v_1 + \Delta m_j$, where $\Delta m_j = j(m_0 - m_j)B_p$, and $j = -1, 0, 1$. For the sake of simplicity, in this paper we assume $m_{-1} = m_1$ and $B_p = 1$, so that $\Delta m_j = j(m_0 - m_j)$.

The circuit equations can be recasted so as to be suited to the numerical simulation by introducing the voltage waves $a(t,z)$ and $b(t,z)$ associated to $v'(t,z)$ and $i'(t,z)$:

$$\begin{cases} v'(t,z) &= a(t,z) + b(t,z) \ , \\ i'(t,z) &= [a(t,z) - b(t,z)]/Z \ . \end{cases} \tag{2}$$

The input characteristic of the transmission line is then

effectively expressed by the constraint:

$$b(t,0) = -a(t-T,0). \tag{3}$$

Since the line variables are considered only at $z = 0$, the z argument will be dropped hereafter.

The equations can also be conveniently normalized by choosing the set of normalized input parameters (θ, h_j, Γ):

$$\theta\frac{d}{d\tau}\tilde{v}(\tau) + \bar{\Lambda}_{Dj}[\tilde{v}(\tau) - E] + (\bar{\Lambda}_{D0} - \bar{\Lambda}_{Dj})j = (1-\Gamma)[\tilde{b}(\tau) - \frac{E}{2}], \quad j = -1, 0, 1 \tag{4}$$

$$\tilde{b}(\tau+1) = \Gamma\tilde{b}(\tau) - \frac{1}{2}(1+\Gamma)\tilde{v}(\tau) \tag{5}$$

where $\tau = t/T$, the tilde indicates functions of τ and j is the region of linear operation at time τ selected by $\tilde{v}(\tau) - E$. The other parameters are defined as follows: $\theta = C/(RT)$, $\zeta = ZG$, $\Gamma = (\zeta - 1)/(\zeta + 1)$,

$$h_j = \frac{(\zeta-1)m_j - G}{(\zeta+1)m_j + G} \quad j = -1, 0, 1 \tag{6}$$

and

$$\bar{\Lambda}_{Dj} = \frac{1}{2}\frac{1-\Gamma^2}{\Gamma - h_j}. \tag{7}$$

For the sake of simplicity, the normalized transmission line impedance ζ is supposed to be positive, so that we have $|\Gamma| < 1$.

Since θ is proportional to C, effects of parasitic C values on the circuit dynamics are studied considering small θ values.

III. Theoretical analysis and discussion

If $C = 0$, *i.e.*, $\theta = 0$, the differential term of (4) vanishes and $\tilde{v}(\tau)$ becomes an algebraic function of $\tilde{b}(\tau)$. In this case, (4) and (5) can be reduced to a nonlinear first order difference equation, *i.e.*, a mapping Φ: $\tilde{b}(\tau) \to \tilde{b}(\tau+1)$, whose properties define the system dynamics.

The family of mappings for the circuit variable $\tilde{b}(\tau)$ is reported here for $E = 0$:

$$\tilde{b}(\tau+1) = h_j\tilde{b}(\tau) + \Delta h_j, \quad j = -1, 0, 1, \tag{8}$$

where $\Delta h_j = j(h_0 - h_j)(1+\Gamma)/[2(\Gamma - h_0)]$. In the above equation, $j = 0$ holds for $|\tilde{b}(\tau)| \le |b_0|$, with $b_0 = (1+\Gamma)/[2(\Gamma - h_0)]$; $j = -1$ holds for $\tilde{b}(\tau) < -b_0$ if $b_0 > 0$ and for $\tilde{b}(\tau) > -b_0$ if $b_0 < 0$; $j = 1$ holds for $\tilde{b}(\tau) > b_0$ if $b_0 > 0$ and for $\tilde{b}(\tau) < b_0$ if $b_0 < 0$.

The stability properties of the fixed points of (8) (those points satisfing $\tilde{b}(\tau+1) = \tilde{b}(\tau)$) depend on the slopes of the mapping Φ, *i.e.*, the parameters h_j. It can be shown that for $|\Gamma| < 1$ (and $E = 0$) no chaotic behavior can be obtained for any value of h_j [5]. A chaotic dynamics of the TDCC with $C = 0$ has been shown in [2] by introducing the voltage generator E.

The behavior of the TDCC is strongly influenced by the presence of the capacitor. If $C \neq 0$ (*i.e.*, $\theta \neq 0$), $\tilde{v}(\tau)$ is a state variable, solution of the first order differential equation (4) having $\tilde{b}(\tau)$ as the source term, and the whole problem is of differential-difference type. In particular, (4) and (5) can be reduced to a first order nonlinear differential-difference equation of neutral type [5].

General results are scarcely available for problems of this kind [2; 4]. In fact, owing to the infinite dimension of the state space, the dynamics of the above equations is unlikely to be described by analytical methods and by standard techniques developed for finite dimensional systems (*e.g.*, Poincaré maps, detection of homoclinic and heteroclinic orbits, etc.). There are, however, two simple tools for a qualitative study of the dynamics of such a system: the detection of the equilibrium points with the analysis of their stability, and extensive numerical simulations.

When the capacitor is added, the equilibrium points do not change, but their stability properties may vary. In fact, in the dynamical case, such properties are determined by the characteristic frequencies (hereafter called eigenvalues) Λ_{kj} of the circuit in each region of linearity j. They are solutions of the characteristic equation below, which is obtained from (4) and (5) by eliminating every source term and looking for a solution of the form $\tilde{b}(\tau) = b_o\exp(\Lambda\tau)$, $\tilde{v}(\tau) = v_o\exp(\Lambda\tau)$, where b_o and v_o are constants and $\Lambda = \Lambda_r + j\Lambda_i$:

$$e^{\Lambda}(\Lambda + \Lambda_{Dj}) = \Gamma(\Lambda + \Lambda_{Nj}), \tag{9}$$

where

$$\Lambda_{Dj} = \bar{\Lambda}_{Dj}/\theta, \quad \Lambda_{Nj} = h_j\Lambda_{Dj}/\Gamma. \tag{10}$$

Equation (9) has infinitely many roots, and it can be shown that it defines a set of eigenfunctions which represents the solution of equations (4) and (5) completely.

A direct parametric analysis of the eigenvalue location is prevented by the lack of an analytical expression for the roots of (9). In order to gain some insight into the effects of the parameter values, we have found the regions of the parameter space where the circuit is stable, *i.e.*, where all the eigenvalues have negative real part. Then, this stability map is used as a guide for a numerical study of the eigenvalue distributions as the parameter space (θ, h_j, Γ) is explored.

In such a parameter space, $C = 0$ corresponds to $\theta = 0$; in this case the stability of the fixed points follows from the h_j values.

For $C \neq 0$ the stability regions can be determined by resorting to Theorems 13.7 and 13.3 reported in [4], and originally stated by S. Pontrjagin. Such theorems give a set of conditions that has to be verified in order to determine the range of the coefficients where all the roots of a polynomial $P(z, \exp(z))$ have negative real part; the application of such results to equation (9) is not trivial and requires a lengthy proof, which leads to the following proposition:

Proposition 1: *In each linear region $\mathcal{R}_j$, all the roots of equation (9) with $|\Gamma| < 1$ have negative real part iff, for any given value of Γ, parameters h_j and θ satisfy $h_j > 1$ and $\theta > \theta_1(h_j)$, or $-1 < h_j < \Gamma$, or $h_j < -1$ and $\theta > \theta_2(h_j)$, where the curves θ_1 and θ_2*

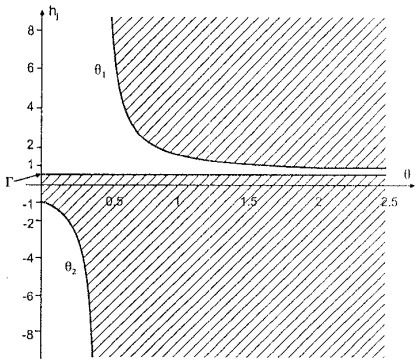

Fig. 3. Stability map in the (h_j, θ) plane for $\Gamma = 0.6$. In the dashed regions all the eigenvalues have a negative real part, while outside the dashed regions at least one eigenvalue has a positive real part.

have the following parametric equation:

$$\begin{cases} \theta = \dfrac{\sin y}{2(\Gamma - y\cos y)} \dfrac{1-\Gamma^2}{\Gamma - h_j} \\ h_j = \dfrac{1 - \Gamma\cos y}{\cos y - \Gamma} \end{cases} \tag{11}$$

and are defined for different ranges of the parameter y:

$$\theta_1 : \quad 0 \le y < \arccos\Gamma \tag{12}$$

$$\theta_2 : \quad \arccos\Gamma < y < \pi. \tag{13}$$

An example of stability map for $\Gamma = 0.6$ is shown in Fig. 3, where points in the dashed areas represent parameter values leading to stable eigenvalues. The value of Γ affects the appearance of the map, but not its structure, which is always composed of two stable areas: one above the level $h_j = +1$ and one below the level $h_j = \Gamma$. Additional characteristic elements of the stability map are the abscissae $\theta_0 = (1+\Gamma)/[2(1-\Gamma)]$ (where the θ_1 curve intersects the $h_j = +1$ boundary) and $\theta_v = \sqrt{1-\Gamma^2}/(2\arccos\Gamma)$ (the vertical asymptote of θ_1 and θ_2).

The stability map offers a first insight into the effects of the capacitor. For $\theta = 0$ (*i.e.*, $C = 0$), the stable region is composed of the segment $|h_j| < 1$ on the h_j axis. When θ takes a finite, non zero value, the point representing the circuit parameters leaves the h_j axis and enters the (θ,h_j) plane. Figure 3 shows that, in this transition, an equilibrium point remains stable if $-1 < h_j < \Gamma$, remains unstable (*i.e.*, at least one eigenvalue has positive real part) if $|h_j| \ge 1$, and switches from a stable to an unstable state if $\Gamma \le h_j < 1$. It is worth remarking that the jump from stable to unstable state happens for any arbitrary small θ.

Furthermore, a transition from unstable to stable state can be obtained for $|h_j| \ge 1$ by large enough capacitors (*i.e.*, by large enough θ values), whereas the equilibrium point remains unstable for any positive value of θ if $\Gamma \le h_j < 1$. As a conclusion, the stability map highlights how the introduction of the capacitor C in the TDCC can completely change its dynamics and points out the importance of parasitic C values for particular combinations of h_j and Γ.

Further information on the eigenvalue distribution can be obtained by the numerical computation of the eigenvalues [7]. The stability map and the numerical analysis carried out in [7] provide a detailed qualitative knowledge of the eigenvalue location for the whole parameter space, allowing to identify the parameter values for which interesting dynamical behaviors are most likely to occur. As an example, they point out that the unstable behavior for $\theta > 0$ and $\Gamma \le h_j \le 1$ is due to a *positive real eigenvalue*. It turns out that this real eigenvalue is proportional to $-\Lambda_{Dj}$ and hence to $1/\theta$; in this case, therefore, the smaller is the capacitance, the stronger is the instability of the equilibrium and the presence of any parasitic capacitance cannot be neglected at all.

A detailed analysis of the eigenvalue distributions for $\theta \neq 0$ and $\theta = 0$ [7] points out that in some cases the displacement of the eigenvalue distributions can be considered a continuous function of θ. In these cases, it is reasonable to conjecture a continuous variation of the dynamics as θ appears. More precisely, we say that, in a region $\mathcal{R}_j$, the eigenvalue distribution for a small value of θ may be considered a continuous evolution of that corresponding to $\theta = 0$ if the eigenvalues Λ_k satisfy $\lim_{\theta\to 0+} \mathrm{Re}[\Lambda_k] = \ln|h_j| \quad \forall k$ (where $\ln|h_j|$ is the real part of the eigenvalues for $\theta = 0$) except for a finite number of eigenvalues Λ_s such that $\lim_{\theta\to 0+} \mathrm{Re}[\Lambda_s] = -\infty$. If the above conditions are not satisfied, we say that there is a discontinuity in the eigenvalue distribution as θ appears, essentially due to a large positive eigenvalue. If for $\theta = 0$ the eigenvalues have also positive real part, we say that the discontinuity takes place with no change of sign (NCS) in the real part; if this is not the case, the discontinuity is accompanied by a change of sign (CS) of the real part. All the possible combinations of h_j values are reported in Tab.1, which points out that if a CS-discontinuity occurs in a region which exhibits a stable equilibrium point, then the dynamic behavior for small θ has an abrupt change with respect to the case $\theta = 0$ (see rows 2, 3, and 4). On the contrary, for $h_0 < \Gamma$ and $h_{\pm 1} < \Gamma$ (see row 1 of Tab. 1), since the eigenvalue distribution varies continuously with θ, we expect a similar dynamic behavior both for $\theta = 0$ and small θ. Both these conjectures have been verified by several simulations.

As an example we report the simulations for a parameter set belonging to row 1 of Tab. 1: $h_{\pm 1} = 0.49$, $\Gamma = 0.60$, $E = 0.78$ and h_0 within the interval $[-4, -1]$. The simulation of the TDCC has been performed by using a Runge-Kutta algorithm with fixed step and starting from a constant initial condition of the type $\tilde{v}(0) = 0.1\,\mathrm{V}$ and $\tilde{b}(\tau) = 0$, $\tau \in]0, 1]$. For $\theta = 0$, the system exhibits the period-adding phenomenon [2]. By assigning a small value to θ, a similar succession of limit cycles, separated by chaotic regions, may be again observed as h_0 is varied. Of course, due to the small but *finite* value of θ, the extension of these regions may vary from that of the case $\theta = 0$. Assuming $\theta = 0.01$, the simulations of the TDCC show a limit cycle of period

Case		eig. distribution		dynamic behavior	
$\mathcal{R}_0$	$\mathcal{R}_{\pm 1}$	$\mathcal{R}_0$	$\mathcal{R}_{\pm 1}$	$\theta = 0$	*small* θ
$h_0 < \Gamma$	$h_{\pm 1} < \Gamma$	C	C	*similar dynamic behavior*	
$\Gamma < h_0 < 1$	$\Gamma < h_{\pm 1} < 1$	CS	CS	*one globally asymptotically stable equilibrium point, belonging either to* $\mathcal{R}_0$ *or to* $\mathcal{R}_{\pm 1}$*, depending on the value of* E	*unstable*
$\Gamma < h_0 < 1$	$h_{\pm 1} > 1$	CS	NCS	*locally stable if there exists one equilibrium point in* $\mathcal{R}_0$*; unstable otherwise*	*unstable*
$h_0 > 1$	$\Gamma < h_{\pm 1} < 1$	NCS	CS	*completely stable, with one or two stable equilibrium points belonging to* $\mathcal{R}_{\pm 1}$	*unstable*
$h_0 > 1$	$h_{\pm 1} > 1$	NCS	NCS	*unstable*	*unstable*

Table 1. Comparison between the eigenvalue distributions and the dynamic behaviors for $\theta = 0$ and for small θ's. The meaning of the achronima are the following: C: continuity; CS: discontinuity with change of sign of the real part; NCS: discontinuity without change of sign of the real part.

$2.2T$ for $h_0 = -1.2$ (Fig. 4(a)); increasing h_0, a chaotic region is encountered and for $h_0 = -2.6$ the chaotic attractor of Fig. 4(b) is observed. A further increase in h_0 reveals a new periodic window; Fig. 4(c) shows the limit cycle of period $4.4T$ obtained for $h_0 = -3.05$. Continuing in increasing h_0, a new chaotic region appears (Fig. 4(d)).

As a concluding remark, we would like to point out that the result presented above is general. In fact, in [2] it is proved that the existence of the period-adding phenomenon requires $h_0 \leq -1$ and $0 \leq h_1 \leq 1$; furthermore, for the mapping Φ to be single-valued, parameters h_j have to satisfy $h_0 < \Gamma$ and $h_{\pm 1} < \Gamma$, or $h_0 > \Gamma$ and $h_{\pm 1} > \Gamma$ [7]. For $|\Gamma| < 1$, the above conditions are equivalent to those of row 1 of Tab. 1, thereby implying the continuity of eigenvalue distributions. This would suggest that *any* TDCC which exhibits the period adding phenomenon for $\theta = 0$, should present a similar dynamics even if a small capacitor is added to the circuit.

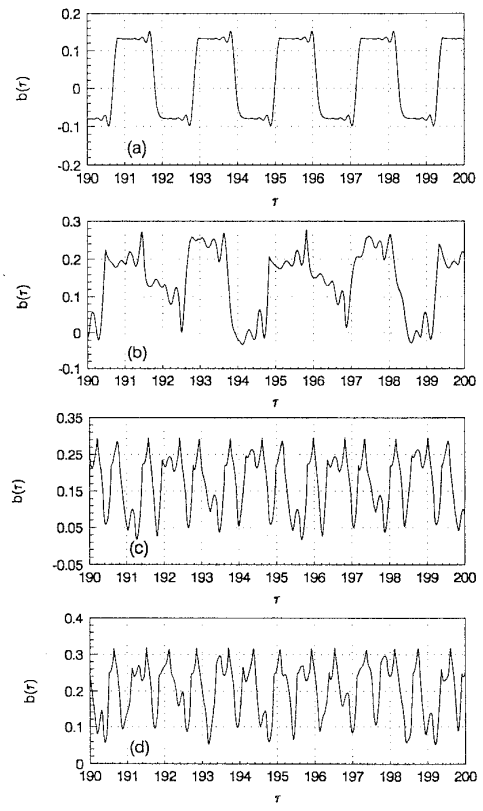

Fig. 4. Capacitor voltage as a function of τ for $\theta = 0.01$ and after a transient of $190T$: (a) periodic attractor of period $2.2T$, $h_0 = -1.2$; (b) strange attractor, $h_0 = -2.6$; (c) periodic attractor of period $4.4T$, $h_0 = -3.05$; (d) strange attractor, $h_0 = -3.9$.

References

[1] Special Issue on Chaos in Nonlinear Electronic Circuits, *IEEE Trans. Circ. and Systems - I*, Vol. 40, 1993.

[2] A.N. Sharkovsky *et al.*, *J. of Circuits, Systems and Computers*, Vol. 3, pp., 645-668, 1993.

[3] A.N. Sharkovsky, *Workshop on Chua's Circuit: Chaotic Phenomena and Applications*, pp. 25-30, in 1993 Int. Symp. on Nonlinear Theory and Its Applications, Hawaii, U.S.A., Dec 5-10, 1993.

[4] R. Bellmann and K.L. Cooke: *Differential-Difference Equations*, New-York Academic Press, London, 1963.

[5] M. Biey *et al.*, *Int. Symp. on Nonlinear Theory and Its Applications*, Hawaii, U.S.A., pp. 803–806, Dec 5–10, 1993.

[6] E. A. Hosny and M. I. Sobhy, *IEEE Trans. Circ. and Systems - I*, Vol. 41, pp. 915–918, Dec. 1994.

[7] M. Biey *et al.*, "Qualitative analysis of the dynamics of the time delayed Chua's circuit", submitted to *IEEE Trans. Circ. and Systems - I.*